The metallophilic interaction between cyclometalated complexes: photobiological applications

Zhou, X.

7

Summary

&

General discussion

&

Outlook

7.1 Summary of this PhD thesis

Cancer is a leading cause of death worldwide. Chemotherapy based on small-molecule drugs is considered as one of the main treatments to fight cancers, though it is accompanied by severe side effects. Nanomedicine and photodynamic therapy (PDT), in this respect, represent emerging alternatives aimed at reducing the side effects of small-molecule drugs. Through rational design, nanocarriers have the reputation to help increasing drug accumulation in the tumor site *via* the enhanced permeability and retention (EPR) effect, which lowers the systemic cytotoxicity of nanoformulated drugs. PDT is a form of light-activated anticancer treatment involving a photosensitizer (usually small molecules), photons, and O_2. This method can selectively activate the drugs in the tumor site to induce cell death, avoiding damage to non-irradiated healthy tissues. However, small-molecule photosensitizers still show some of the drawbacks of chemotherapy, such as low tumor accumulation and rapid blood clearance. For example, padeliporfin (Tookad®, a clinical approved palladium-based photosensitizer) reaches it highest plasma concentration in the human body at as fast as 5 min, and it is then rapidly metabolized by kidneys.[1] In this thesis, PDT and nanomedicine were combined in order to achieve efficient accumulation of photosensitizers within cancer cells (*in vitro*) or at the tumor site (*in vivo*), before being selectively activated by light irradiation. We propose an alternative to the complicated synthesis and challenging reproducibility of multi-components nanocarriers, which often lead to low drug loading efficiencies and dramatically restrict clinical applications of nano-sized drug delivery systems that, in pre-clinical tests, had appeared as promising. In the research described in this thesis, we focused on the design and preparation of small-molecule photosensitizers based on tetradentate ligands cyclometalated to d^8 transition metal centers. We realized that these molecules can be used to develop a molecular photosensitizer self-assembly nanosystem (MoPSAN) based on the supramolecular assembly of these molecules *via* the metallophilic metal...metal (M…M) interaction. These nanosystems achieve high drug-loading, high cellular uptake *in vitro* and high tumor accumulation efficiency *in vivo*, and excellent anticancer PDT effects, both *in vitro* and *in vivo*.

In **chapter 2**, we describe the two isomers of a cyclometalated palladium(II) complex and compared their anticancer PDT properties *via* several photophysical and photobiological methods. The first isomer **PdL^1**, which shows an N^N^C^N coordination mode, showed excellent singlet oxygen generation quantum yield (0.89) under blue light irradiation, resulting in high blue-light-activated photoindexes in human cancer cells. By contrast, the second isomer **PdL^2**, characterized by an N^N^N^C coordination mode, had both low blue light absorption

and low singlet oxygen quantum yield (0.38), giving a negligible activation by blue light *in vitro*. DFT calculation showed that the higher absorption in the blue region of **PdL^1**, and thus its lower HOMO-LOMO energy gap, was due to the closer proximity between the electron-rich cyclometalated aromatic cycle and the nitrogen bridge of the ligand, while in **PdL^2** both aromatic rings adjacent to the amine bridge are electron-poor pyridine rings, which lowers the HOMO energy. These results demonstrate that changing the position of the carbon-metal bond in the coordination sphere of photoactive organometallic prodrugs can be used to tune the energy gap between their frontier orbitals, and hence their absorption in the visible region of the spectrum, which is essential in PDT applications.

The deprotonation of the non-coordinated NH bridge in the palladium complexes described in **chapter 2** resulted in water-insoluble neutral metal complexes, thus limiting their application for cancer treatment *in vivo*. In **chapter 3**, we describe the results of methylation of the amine bridge to avoid this problem. Three water-soluble analogous palladium complexes were successfully synthesized: two cyclometalated isomers **[PdMeL^1]OAc** (N^N^C^N coordination) and **[PdMeL^2]OAc** (N^N^N^C coordination), and a reference tetrapyridyl complex **[Pd(Mebbpya)](OAc)$_2$** (N^N^N^N coordination). All complexes are soluble in pure water. **[PdMeL^1]OAc** has similar photophysical and photobiological properties compared with **PdL^1**, and even showed good blue-light activated PDT effect in a mice tumor xenograft, suggesting the promising potential of palladium-based photosensitizers for PDT application. Critically, in this work we found that cyclometalation of a palladium complex triggers the self-assembly of the complex into nanorods *via* the metallophilic Pd…Pd interaction, which also depends on the presence of proteins in the cell medium used to dissolve the compounds. Importantly, endocytosis plays a critical role in the cellular uptake of these aggregates, and it promotes much higher cellular uptake of the cyclopalladated complexes than conventional non-cyclometalated tetrapyridyl analogue **[Pd(Mebbpya)](OAc)$_2$**. The role of the protein corona in drug delivery systems is actively debated for several years, but the nanoscale, protein-dependent self-aggregation of a self-assembling drug molecule, had not been documented before. Overall, this work shows that (pro)drugs that self-assemble into nanorods can lead to excellent drug penetration in 3D tumor models, which suggests a new strategy to combine metallodrugs with nanomedicine, further discussed in **chapter 5**.

In the research described in **chapter 4**, using the same ligands described in **chapter 3**, but changing the metal, we demonstrated that platinum(II) complexes **[PtMeL^1]OAc** and **[PtMeL^2]OAc** both showed strong metallophilic interactions, which also resulted in the self-

assembly of nanoaggregates in cell-growing medium. However, although both series of complexes (with Pd^{2+} or Pt^{2+}) showed self-assembly *via* metallophilic interactions and cell-dependent cytotoxicity in the dark, their photochemical properties were found to be dramatically different. The excellent PDT properties and negligible emission of the palladium aggregates were replaced, in the platinum series, by poor PDT properties but red-shifted absorption and deep-red emission properties, which allows for using these aggregates in cell imaging rather than for phototherapy. The different photochemical properties of the platinum *vs.* palladium complexes must originate from their different relative rates of excited state deactivation, both in the self-assembled and monomeric forms. Phosphorescence and non-radiative deactivation to the ground singlet state are quantum-chemically forbidden processes that strongly depend on spin-orbit coupling, which is stronger for platinum(II) than for palladium(II) ions. Generally, Pt(II) $5d_z^2$ orbital is higher in energy than the Pd(II) $4d_z^2$ orbital, which leads to Pt(II) showing a stronger influence than Pd(II) in the frontier molecular orbitals, inter-system crossing efficiency and the $T_1 \rightarrow S_0$ radiative decay, altogether giving platinum complexes a more intense phosphorescence.[2] This phosphorescence, located in the deep-red region of the spectrum, allowed us to study the uptake and localization of these supramolecular nanoparticles in cells; in A549 cells the deep-red emissive nanoaggregates of **[PtMeL^2]OAc** were located in the mitochondria, which was also confirmed by cell electron microscopy due to the high electron density of platinum compounds. Overall, this set of polypyridyl platinum complexes demonstrated new perspectives in using the metallophilic interactions to build supramolecular nanosystems that, at high concentration, can kill cancer cells, but at low concentration, may be used as deep-red trackers for different organelles – here the mitochondria.

In **chapter 5**, we describe a bis-cyclometalated palladium complex, **PdL^3**, which allowed on the one hand for further shifting the absorption of the complex towards longer wavelengths, and on the other hand, for further decreasing the charge to form a neutral complex and generating strong Pd…Pd interactions. **PdL^3** was indeed demonstrated to self-assemble as nanoaggregates in cell-growing medium, but also to have improved PDT properties compared to the mono-cyclometalated complex **PdL^1**: next to being activated with green light instead of blue light due to the further destabilization of the HOMO by the second Pd-C bond, it was also particularly cytotoxic under hypoxic conditions, with photoindexes of up to 70 in skin melanoma cell lines. This excellent reactivity was due to a PDT type I mechanism, which is notoriously less dependent on the O_2 concentration than PDT type II. **PdL^3** served as a proof-of-concept for the MoPSAN concept, where a PDT photosensitizer self-assembles into

nanostructures for tumor targeting *in vivo* using the EPR effect. Dense nanoparticles were found by electron microscopy (EM) in plasma following intravenous injection of the compound in mice, which demonstrates self-assembly in biological conditions. Then, ICP-MS measurements demonstrated the significant accumulation of **PdL^3** in the tumor, with exceptional drug delivery efficacy of up to 10.2% ID/g. EM images of tumor slices proved again the accumulation of self-aggregated nanoparticles of **PdL^3** in the solid tumor. With these results in hand, we advocate that the supramolecular metallophilic Pd…Pd interaction has a high potential 1) to build supramolecular nanocarriers with improved tumor accumulation *via* the EPR effect, and 2) to generate PDT photosensitizers that conserve their phototoxic properties under hypoxia.

Finally, in **chapter 6** we report the chemistry of cyclometalated Au(III) compounds. Although Au(III) is isoelectronic to Pt(II), it has significantly different properties due to its higher charge and electronegativity (2.4 for Au and 2.2 for Pt). In general, cyclometalation in polypyridyl metal complexes decreases their molecular charge, compared with conventional nitrogen coordination, which significantly influences their lipophilicity as well. As discussed in **chapter 2**, many reports claim that the higher lipophilicity of cyclometalated complexes stimulates their cellular uptake *via* passive transport through the cell membrane, which potentially may lead to better therapeutic effects with lower doses of a compound, but at the cost of cancer selectivity. On the other hand, cyclometalation stabilizes the Au(III) oxidation state, which lowers the propensity of cyclometallagold compounds to be reduced by biological thiol groups once they have reached the cytosol. We investigated the coordination of a pair of tetrapyridyl ligands to gold(III) ions and in **chapter 6** describe the serendipitous discovery that one of these ligands preferentially binds the Au(III) center *via* "rollover cyclometalation" to form a bis-cyclometalated gold(III) complex **[Au(biqbpy1)]Cl** (C^N^N^C), while the other ligand coordinates with its four nitrogen atoms to afford the traditional tetrapyridyl complex **[Au(biqbpy2)]Cl** (N^N^N^N). Interestingly, both cationic complexes bear the same +1 charge due to the deprotonation of the amine bridges in **[Au(biqbpy2)]$^+$**, while the bis-cyclometalated analogue **[Au(biqbpy1)]$^+$** keeps its amine bridges protonated. These two isomers offer hence the unique opportunity to compare cyclometalated *vs.* non-cyclometalated Au(III) complexes without a change of the overall charge of the complex. We found that the roll-over cyclometalated **[Au(biqbpy1)]Cl** is highly stable in reducing biological conditions, but that it also forms nanoparticles in cell medium, which led to a 6-fold more efficient uptake in A549 cancer cells, compared with the tetrapyridyl analogue **[Au(biqbpy2)]Cl** that does not form nanoparticles but is much more prone to decomposition by reduction in cell-growing medium.

The identical charge, but different aggregation properties of **[Au(biqbpy1)]Cl** *vs.* **[Au(biqbpy2)]Cl**, give a new perspective on the enhanced cellular uptake of cyclometalated gold complexes. As unambiguously demonstrated for Pd(II) and Pt(II) cyclometalated complexes reported in previous **chapters** of this thesis, these nano-aggregates may trigger active transport such as endocytosis, which is typically more efficient than passive transport. Moreover, **[Au(biqbpy1)]Cl** is more stable in biological conditions and hence showed decreased TrxR inhibition, compared with **[Au(biqbpy2)]Cl** which upon intracellular reduction released the known TxrR-inhibiting Au^{+} as free ions. The resulting cytotoxicity to cancer cells was lowered for **[Au(biqbpy1)]Cl** compared with **[Au(biqbpy2)]Cl**, but its toxicity to non-cancerous cells was also comparatively much lower, i.e., its selectivity to cancer cells was higher than that of **[Au(biqbpy2)]Cl**. Meanwhile, both complexes exhibited similarly high potassium channel binding ability, which might be due to their identical charge and similar molecular shape. Their potassium channel binding ability was also higher than that of the tetrapyridyl ligands they were made of, suggesting that metal complexation might be an alternative method to regulate the potassium channel activity of small molecules. Altogether, the comparison of these isomers, from a chemical and biological point of view, provided new insights on the use of cyclometalation as a drug design principle to modify the balance between stability, aggregation, toxicity, and protein inhibition properties of gold(III) anticancer complexes.

7.2 General discussion

7.2.1 Cyclometalation reactions

Overall, we have reported in this thesis several cyclometalated polypyridyl complexes based on palladium(II), platinum(II) and gold(III), and compared their chemical and biological properties with that of their classical nitrogen-coordinated analogues. cyclometalatedC-H activation in cyclopalladation reactions usually involve either tetrachloridopalladate salts in presence of a base, or palladium acetate in acetic acid or benzene.[3] All the cyclometalated palladium complexes reported in this thesis have been obtained by the reaction of palladium acetate and the corresponding ligands in refluxing acetic acid. A similar method also was successful for most cyclometalated platinum complexes, which were mostly obtained by using bis(acetylacetonate)platinum(II) as a precursor. However, three unexpected cyclometalated Ru(III), Au(III) Pd(II) and Pt(II) complexes were also obtained, which are shown in Figure 7.1 but have not been described in this thesis. The compounds **[Ru(MeL^{1})Cl$_2$]**, **[Au(HL^{2})Cl](AuCl$_4$)**, **[PdL^{4}OAc]** and **[Pt(L^{5})Cl]**, were obtained *via* the reaction of

dichloro(*p*-cymene)ruthenium(II) dimer, $NaAuCl_4$, $Pd(OAc)_2$, and K_2PtCl_4, respectively, with the corresponding ligands in refluxing acetic acid. It should be noticed that the Ru(II) precursor was oxidized to Ru(III) in the cyclometalation process, even under argon, indicating that the thermodynamic stability of cyclometalated Ru(III) complexes might be high enough, at least in such conditions, to hinder the synthesis of cyclometalated Ru(II) complexes based on this ligands. In the three complexes **[Au(HL^2)Cl](AuCl$_4$)**, **[PdL^{4}OAc]** and **[Pt(L^5)Cl]**, the compound obtained was not the expected one but the oxidation state of the metal did not change during cyclometalation (Figure 7.1). In that regard, these cases are similar to the rollover cyclometalated **[Au(biqbpy1)]Cl** described in **chapter 6**: upon reacting $HAuCl_4$ with **H$_2$biqbpy1** in refluxing methanol, the obtained cyclometalated compound did not correspond to the expected tetrapyridyl coordination mode.

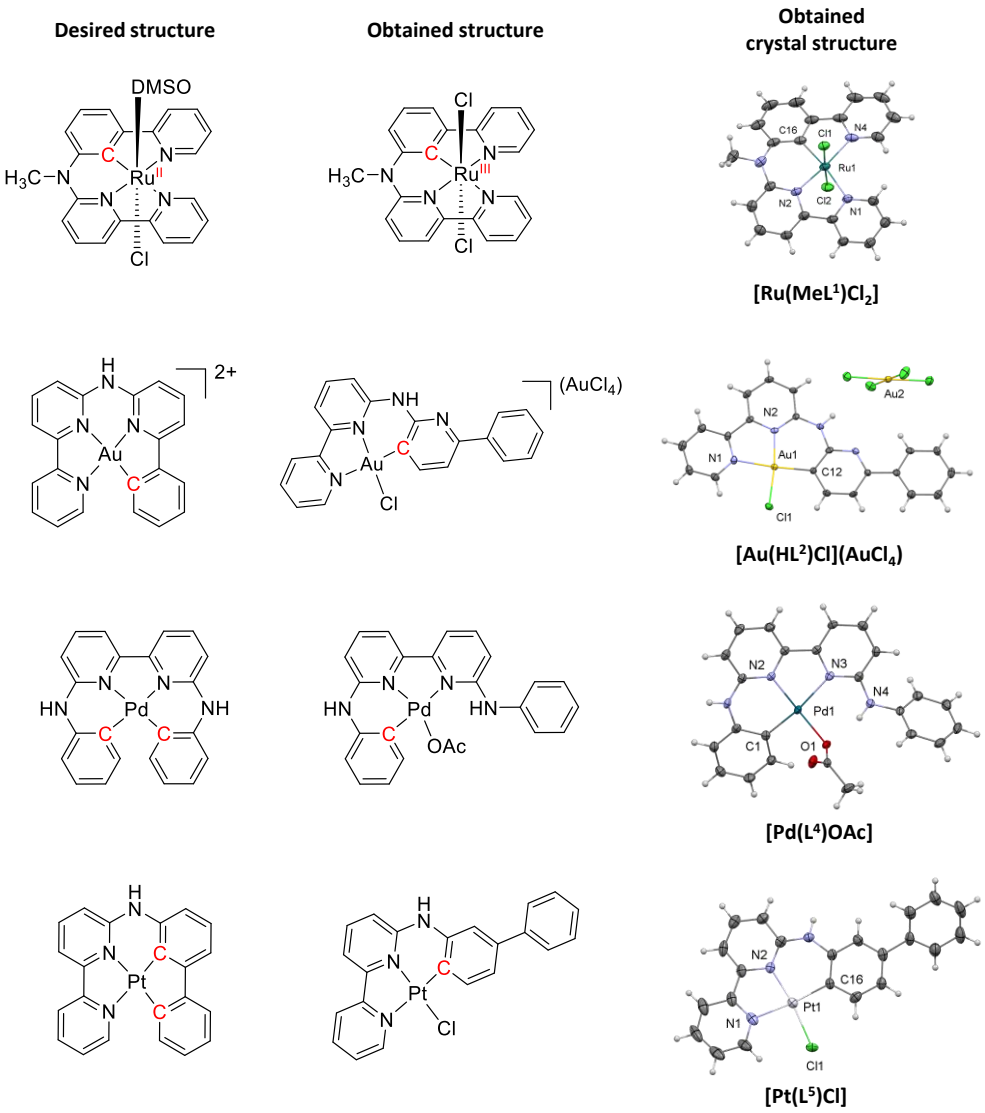

Figure 7.1 *The chemical and crystal structures of unexpected cyclometalated complexes obtained in our research, but not described in great details in this thesis.*

It is hence particularly interesting to illustrate the different possible outcomes of a cyclometalation reaction, with a tetradentate ligand, by comparing the structures of **[PdL^2]** described in **chapter 2** and **[Au(HL^2)Cl](AuCl$_4$)** (Figure 7.1). The ligand is the same, but different metal precursors resulted in different cyclometalated products. As shown in Figure 7.2, the acetate or choride anions are also potential ligands, which may play a blocking role towards binding of the expected nitrogen ligands to the metal center. On the other hand, these same ligands may activate a C-H on the same pyridine ring *via* intramolecular O…H or Cl…H hydrogen bond, ultimately promoting the formation of Pd-C or Au-C bonds. The $Pd(OAc)_2$ precursor in particular was prone to such C-H activation of phenyl groups, as acetates are rather basic and weak ligands (Figure 7.2a). For the gold precursor $NaAuCl_4$, the chloride ligand is probably a better ligand than acetate, while the C-H…Cl intramolecular hydrogen bond may be less strong due to the lower basicity of chloride, compared to acetate; hence coordination of the pyridine ring and C-H activation of the terminal phenyl group was slower, compared to the activation of the more acidic pyridine C-H bond, which further triggered a "rollover" (Figure 7.2b) similar to that described in **chapter 6**. The proposed intermediates for the rollover cyclometalation observed for **[Au(HL^2)Cl]$^+$** are shown in Figure 7.2c. Interestingly, when reacting $PtCl_4^{2-}$ with **HL^5** the complex **[Pt(L^5)]$^+$** shown in Figure 7.1 was obtained, which is very similar to **[Au(HL^2)Cl]$^+$**. This result suggested that the nature of the ancillary ligand on the metal precursor (acetate *vs.* chloride), and notably its basicity and ability to bind to the metal, play a more essential role on the final outcome of the cyclometalation reaction, that played by the electron-richness of the aromatic cycle that finally becomes cyclometalated (pyridine vs. phenyl group).

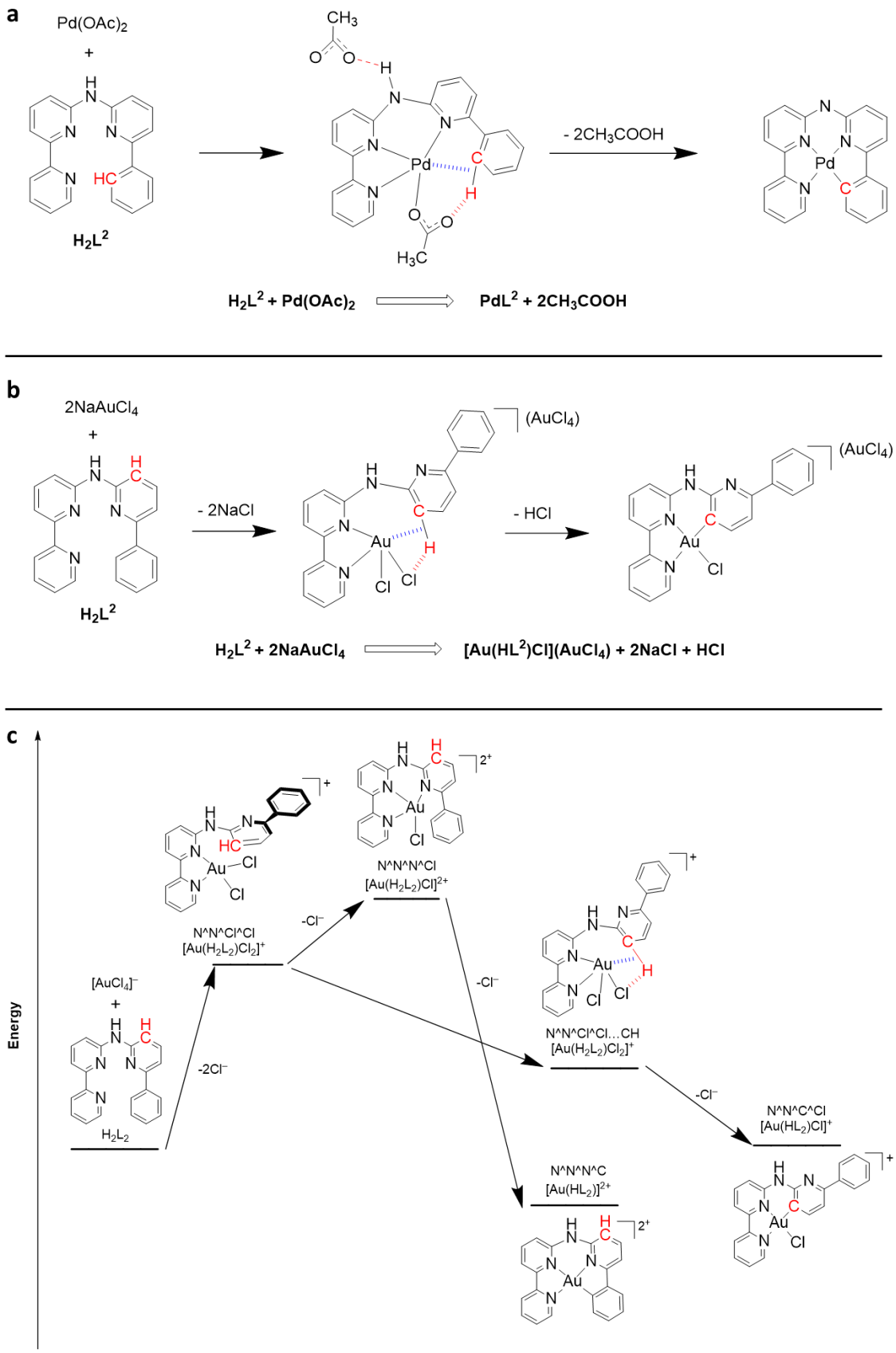

Figure 7.2 *Proposed cyclometalation mechanism for* ***PdL²*** *(a),* ***[Au(HL²)Cl](AuCl₄)*** *(b) and proposed reaction intermediates towards the preparation of* ***[Au(HL²)]²⁺*** *(c).*

7.2.2 Supramolecular aggregation of cyclometalated complexes in a biological context

In this thesis it is reported that cyclometalated polypyridyl metal complexes always showed better cellular uptake than their tetrapyridyl analogues, which is usually attributed, in the recent literature, to the higher lipophilicity of the former and their enhanced ability to cross membranes by passive diffusion. However, we demonstrated that actually the nanoaggregation of cyclometalated complexes triggers efficient active endocytic transport of the compound, rather than passive transport through the cell membrane. This research indicates the critical importance of understanding the supramolecular behavior of anticancer compounds in cell-growing medium, *i.e.* before they interact with living cells. Gasser' group recently reported the nanoaggregation of several ruthenium complexes in aqueous solutions,[4] and also emphasized that understanding the nature of the actual metal species entering cancer cells is critical. We envision that the present work has clearly demonstrated that nanoaggregation in cell medium and in blood has impressive consequences on the cellular uptake mechanism and efficiency of drug penetration into tumors *in vivo*. With this knowledge, the formation of nanoaggregates should be taken into serious consideration, and even consciously applied for the future development of metallodrugs.

7.3 About the strength of the metallophilic interaction

We demonstrated that cyclometalation is a convincing method to stimulate supramolecular metallophilic M...M interactions of Pd(II) and Pt(II) complexes and their subsequent self-assembly to nanoaggregates in biological media. The M-C bond of cyclometalated complexes decreases the positive charge of the complex, which combined with the strong π-π stacking interactions of planar tetradentate aromatic ligands allows these metal centers to overcome their electrostatic repulsion, resulting in overlapping of metal-based d_z^2 orbitals and ligand-based π orbitals with those of nearby complexes. The metallophilic interaction was initially described for Au(I) species, and was therefore called an aurophilic interaction.[5] However, in recent literature it was revealed that also Au(III), Pt(II), and Pd(II) complexes may show metallophilic M...M interactions.[6] Although the torsion of the **biqbpy1**$^{2-}$ and **biqbpy2**$^{2-}$ ligands described in **chapter 6** appeared too large to generate a short Au…Au distance, it may be interesting to compare the influence of the nature of the d^8 metal on the strength of the metallophilic interaction. In order to do so, we calculated the structures of dimers of two series of analogous Pd(II), Pt(II), and Au(III) complexes. In the first series, the ligand **HMeL^1** was used, which is a phenyl derivative of the tetrapyridyl ligand **Mebbpya**. It should be noted that **[Pd(MeL^1)]**$^+$, **[Pt(MeL^1)]**$^+$, and **[PdMebbpya]**$^{2+}$ were all synthesized and are described in this thesis

(**chapter 3**), while **[Au(MeL^1)]$^{2+}$** has not been synthesized yet. DFT models of these dimers and their monomer were minimized in vacuum using PBE0 as functional and the dDsC correction to take into account dispersion effects. As shown in Figure 7.3a, dimers of the monocationic complexes **[Pd(MeL^1)]$^+$** and **[Pt(MeL^1)]$^+$** exhibit short M…M distances (around 3.18-3.34 Å), while for the bicationic analogues **[Au(MeL^1)]$^{2+}$** and **[Pd(Mebbpya)]$^{2+}$** the minimization jobs diverged to Au…Au and Pd…Pd distances longer than 5 Å, at which no metallophilic interaction can be considered anymore. This theoretical result indicated that the reduction of the charge of Pd(II), Pt(II) or Au(III) complexes by cyclometalation is one of the main reasons why the metallophilic interaction may arise: cationic metal complexes repulse each other by electrostatic effects, and this charge repulsion must be overcome to trigger self-assembly *via* the metallophilic M...M interactions.

To further study the influence of the charge of the monomer on the formation of dimers, and exclude the influence of a particular ligands, DFT calculations were also carried out for the biscyclometalated analogues of the complexes described in the previous paragraph, *i.e.* neutral **[Pd(MeL^3)]**, **[Pt(MeL^3)]**, and monocationic **[Au(MeL^3)]$^+$**. As shown in Figure 7.3b, calculations of the dimer **{[Au(MeL^3)]}$_2^{2+}$** did converge this time, with a short Au…Au distance (3.45 Å) demonstrating the importance of charge control for the generation of M...M interactions. The neutral dimers **[Pd(MeL^3)]$_2$** and **[Pt(MeL^3)]$_2$** also showed short M…M distances (3.17 and 3.20 Å, respectively), suggesting that experimentally these three complexes may generate metallophilic M...M interactions (see also **chapter 5** for an example with palladium and **HL^3**). We also calculated the stabilization energy $\Delta E_{M...M}$ of all three M…M dimers, defined as $\Delta E_{M...M}$ = total bonding energy of the dimer – 2× total bonding energy of monomer. $\Delta E_{M...M}$ was the highest for **[Pt(MeL^3)]** ($\Delta E_{Pt...Pt}$ = -126.0 kJ/mol), very closely followed by **[Pd(MeL^3)]** ($\Delta E_{Pd...Pd}$ = -123.6 kJ/mol). Both values are of the same order of magnitude compared to hydrogen bonds, as the strongest hydrogen bond FH..F$^-$ is -169 kJ/mol.[7] By contrast, the gold(III) dimer was found to be higher in energy than the two monomers, with $\Delta E_{Au...Au}$ = +68.34 kJ/mol, highlighting again the destabilizing effect brought by the higher charge of the trivalent gold(III) center, compared to divalent metal centers (Figure 7.3c). These data suggest that the metallophilic Pd…Pd and Pt…Pt interactions help to stabilize these dimers, while the aurophilic Au…Au interaction (at least in this complex) is not strong enough to stabilize the dimer **{[Au(MeL^3)]}$_2^{2+}$**. For such a molecule supramolecular aggregates based on the aurophilic interaction would require some additional attracting interaction, for example with counter anions or proteins from the medium, which have not been introduced in this model.

Altogether, according to DFT calculations the charge of d^8 metal complexes based on Pd(II), Pt(II) and Au(III) strongly influence the generation of metallophilic M...M interaction, and in both series the Pt(II)…Pt(II) and Pd(II)…Pd(II) interactions were comparable in energy, while the Au(III)…Au(III) interaction was found the weakest. This result also matches well with the popularity of the metallophilic M...M interaction in the scientific literature, where studies on metallophilic interaction of Pt(II) and Pd(II) compounds are rather common, while those related to Au(III) complexes remain scarce.[6, 8]

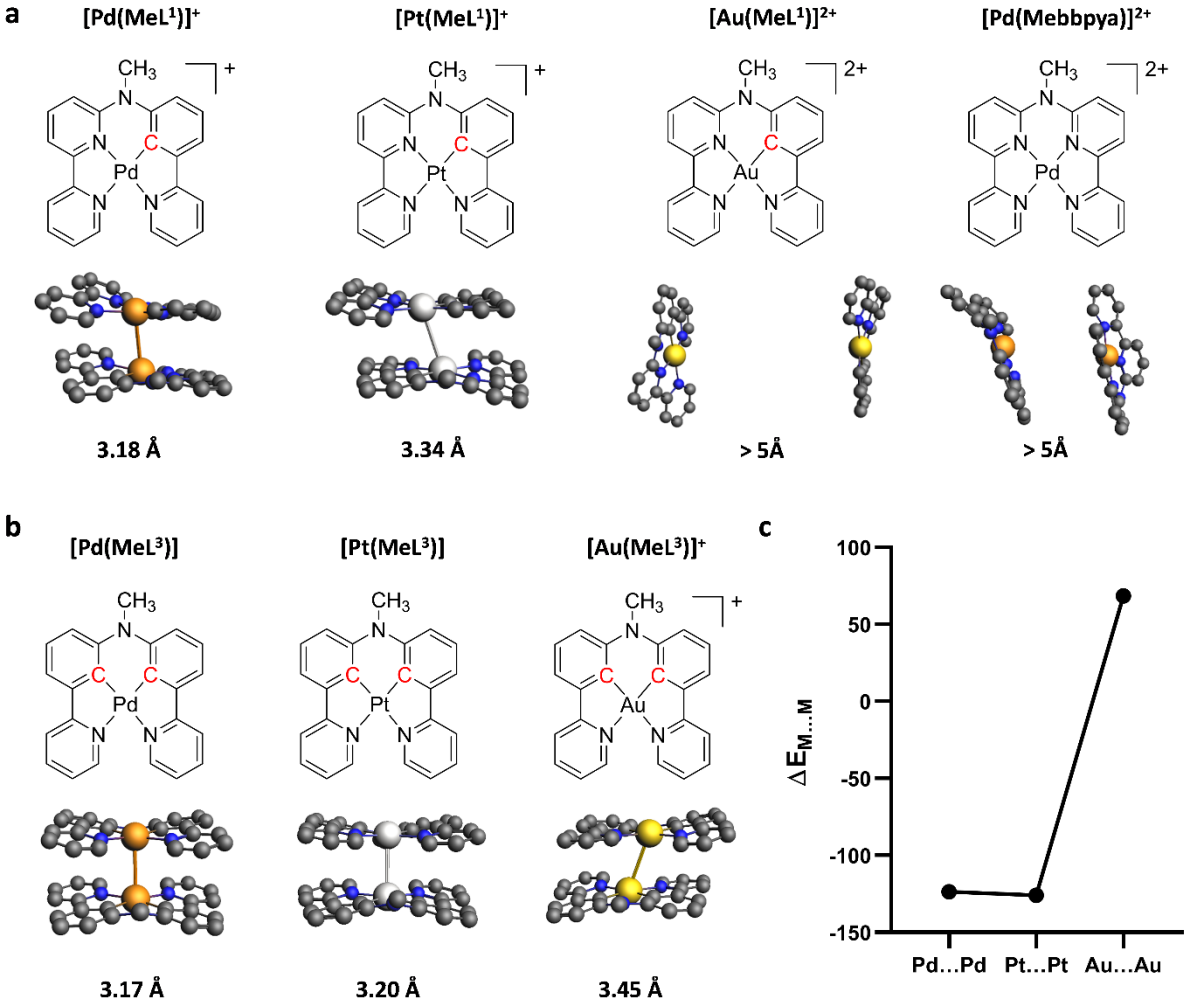

Figure 7.3 *(a) DFT structures and M…M distances (Å) for the minimized dimers of* ***[Pd(MeL^1)]$^+$****, and* ***[Pt(MeL^1)]$^+$****. For* ***[Au(MeL^1)]$^{2+}$*** *and* ***[PdMebbpya]$^{2+}$*** *the M…M distances diverged above 5 Å. (b) Chemical formulae, DFT-minimized structures, and M…M distances (Å) for the dimers of* ***[Pd(MeL^3)]****,* ***[Pt(MeL^3)]*** *and* ***[Au(MeL^3)]$^+$****. (c) DFT-calculated stabilization energy $\Delta E_{M...M}$ for the M…M interaction in* ***[Pd(MeL^3)]$_2$****,* ***[Pt(MeL^3)]$_2$*** *and* ***{[Au(MeL^3)]}$^{2+}$****. Level of theory: ADF/PBE0-dDsC/TZP in vacuum with scalar (ZORA) relativistic effects.*

7.3 Outlook

In this thesis, we describe that cyclometalated palladium complexes can be made that have interesting PDT efficiency following type I or type II mechanisms as supramolecular aggregates, while analogous cyclometalated platinum complexes also aggregate strongly via the metallophilic Pt…Pt interaction, but show poor photodynamic properties. Instead, aggregation makes them strongly emissive in the photodynamic window of the spectrum, thus allowing deep-red bioimaging application. To combine the PDT properties of cyclopalladated complexes and the bioimaging potential of cycloplatinated complexes, it might be possible to foresee the use of mixtures of both molecules, to generate self-assemblies *via* heterometallic Pd…Pt…Pt interactions. With such mixtures new theranostic nanoplatforms capable of PDT and cell imaging are around the corner for fighting cancer, in which the Pd species play the role of a PDT agent, while the Pt…Pt species emerge as deep-red trackers.

We also demonstrated the stability of these supramolecular metallophilic M...M interactions in solution, in living cells, and even in living mice. The resulting nanostructures with both types of cyclometalated complexes are strongly dependent on the proteins contained in the aqueous solution transporting the compound, whether it is cell-growing medium or circulating blood in mice. We found that the nanoparticles formed *via* Pd…Pd interaction show an extraordinary tumor accumulation efficiency, suggesting the promising potential of such aggregated metal complexes to develop nanocarrier systems based on the metallophilic M...M interaction. For example, it would be possible to conjugate some tumor-microenvironment-sensitive medicinal components to the bridging amine group of palladium or platinum cyclometalated complexes, and let the metallophilic M...M interaction drive nanoparticle formation in the living body and target these nanoparticles to the tumor. Following tumor uptake, the medicinal components would be released or activated, to achieve the targeted treatment.

In this thesis, we have reported the influence of the nature of the metal center on the photochemical and photobiological properties of metal complexes based on one tetradentate ligand structure. Next to the compounds reported in **chapters 2-6**, we also synthesized two biscyclometalated palladium and platinum complexes **[PdL^6]** and **[PtL^6]** (Figure 7.4), the detailed study of which has not been included in this thesis. These compounds showed intricate phosphorescence properties that are also tuned by the metal center, the ligand, and the self-assembly of the molecule. When dissolving **[PdL^6]** or **[PtL^6]** in pure DMSO, deep-blue or green

emission was observed, respectively, which were attributed to the monomers. However, upon increasing the water faction in DMSO (f_w = volume of water/total volume) from 0.0 to 0.9, the two complexes aggregated, to generate the metal…metal interaction, as demonstrated by a significant red-shift of the emission. These complexes hence show interesting properties as luminescent materials, though time was too short to evaluate them comprehensively.

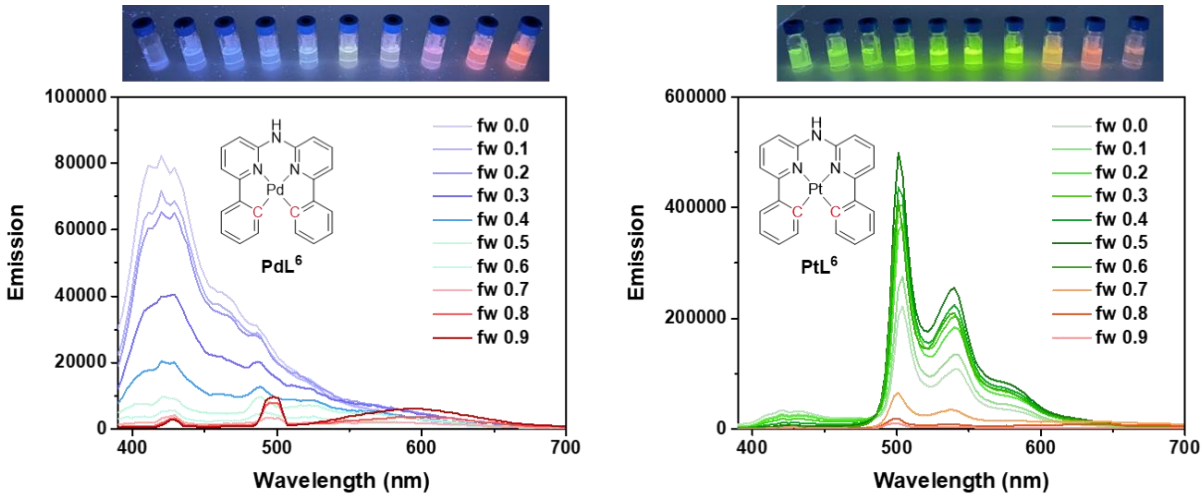

Figure 7.4 *Visual impression and emission spectra of* ***[PdL^6]*** *and* ***[PtL^6]*** *in water/DMSO mixtures (f_w change from 0.0 to 0.9).*

In conclusion, the results described in this thesis bridge the fields of anticancer metallodrugs, photodynamic therapy, cell imaging, luminescent materials, and nanomedicine. By using cyclometalation and the supramolecular metallophilic M...M interaction, it was possible to show the fantastic impact that metal complexes may have on the development of future anticancer drugs and nanomaterials.

7.4 References

1. J. Trachtenberg, A. Bogaards, R. A. Weersink, M. A. Haider, A. Evans, S. A. McCluskey, A. Scherz, M. R. Gertner, C. Yue, S. Appu, A. Aprikian, J. Savard, B. C. Wilson and M. Elhilali, *J. Urol.*, 2007, **178**, 1974-1979.
2. Q. Wan, W.-P. To, X. Chang and C.-M. Che, *Chem*, 2020, **6**, 945-967.
3. J. Dupont, C. S. Consorti and J. Spencer, *Chem. Rev.*, 2005, **105**, 2527-2572.
4. A. Notaro, G. Gasser and A. Castonguay, *ChemMedChem*, 2020, **15**, 345-348.
5. Z. Wu, Y. Du, J. Liu, Q. Yao, T. Chen, Y. Cao, H. Zhang and J. Xie, *Angew. Chem. Int. Ed.*, 2019, **58**, 8139-8144.
6. Q. Wan, J. Xia, W. Lu, J. Yang and C. M. Che, *J. Am. Chem. Soc.*, 2019, **141**, 11572-11582.
7. J. Emsley, *Chem. Soc. Rev.*, 1980, **9**, 91-124.
8. C. Zou, J. Lin, S. Suo, M. Xie, X. Chang and W. Lu, *Chem. Commun.*, 2018, **54**, 5319-5322.